

Fermi National Accelerator Laboratory

FERMILAB-FN-665

**Preliminary Report on the Time Dependent Effects Observed in the
E853 Channeling Extraction Experiment at the Tevatron**

R.A. Carrigan, Jr.

*Fermi National Accelerator Laboratory
P.O. Box 500, Batavia, Illinois 60510*

March 1998

Disclaimer

This report was prepared as an account of work sponsored by an agency of the United States Government. Neither the United States Government nor any agency thereof, nor any of their employees, makes any warranty, expressed or implied, or assumes any legal liability or responsibility for the accuracy, completeness, or usefulness of any information, apparatus, product, or process disclosed, or represents that its use would not infringe privately owned rights. Reference herein to any specific commercial product, process, or service by trade name, trademark, manufacturer, or otherwise, does not necessarily constitute or imply its endorsement, recommendation, or favoring by the United States Government or any agency thereof. The views and opinions of authors expressed herein do not necessarily state or reflect those of the United States Government or any agency thereof.

Distribution

Approved for public release; further dissemination unlimited.

Preliminary Report on the Time Dependent Effects Observed in the E853 Channeling Extraction Experiment at the Tevatron¹

R. A. Carrigan, Jr.²,
Fermi National Accelerator Laboratory, Batavia, Illinois 60510

Abstract

Time dependent effects in the E853 crystal extraction experiment have provided interesting insights into several crystal extraction and accelerator beam halo phenomena. In kick mode the observed turn-to-turn time structure was governed by accelerator beam dynamics. Kick mode extraction was reasonably modeled by simulation programs except that extraction persisted longer than predicted and so-called wrong side turns rapidly came into equilibrium with right side turns, possibly because of non-linear effects in the accelerator. Moving the crystal and collimators provided information on the diffusion rate of the halo. Among the most interesting time dependent observations was the behavior of the extracted signal from the Tevatron flying wires. Particles interacting with the wires were extracted with high efficiency. A distinct feature of the flying wire data was a delayed high-yield portion that extended for tens of milliseconds.

1. Introduction

E853 at Fermilab was designed to study beam extraction with bent crystal channeling in the TeV regime. The goals included extracting one million 900 GeV/c protons/second with 10^{12} protons circulating in the Tevatron, studying the extraction efficiency, showing that the luminosity lifetime of the circulating beam was not adversely affected, and investigating the backgrounds created at the two Tevatron collider experiments. In the course of these investigations considerable information was accumulated concerning time-dependent effects in the Tevatron.

¹ This preliminary report contains background information for a more comprehensive E853 article in preparation. It is being released in this form as a vehicle for discussion and because of possible relevance to C0 work.

² The other members of the E853 collaboration are S. Baker (ANL), D. Chen and A. McManus (AT&T), S. Ramachandran (BACG), D. Cline, J. Rhoades, and J. Rosenzweig (UCLA), G. Jackson, N. Mokhov, and T. Murphy (FNAL), A. Asseev and V. Biryukov (IHEP), A. Taratin (JINR), A. Bogacz (JNAF), V. Golovatyuk (Lecce), J. A. Ellison (New Mexico), A. Khanzadeev, T. Prokofieva, V. Samsonov, and G. Solodov (PNPI), E. Tsyganov (Southwestern Medical Center), B. Newberger (Texas), H.-J. Shih (Affiliated Computer Services), W. Gabella (Vanderbilt), and B. Cox (Virginia).

A wide variety of time-dependent effects were observed in the course of E853. Characteristic time constants ranged from tens of microseconds to many seconds. Some were inextricably related to the nature of channeling such as multi-turn processes where some fraction of the beam on an incorrectly aligned crystal multiply-scattered to an aligned angle. Others like the behavior of the extracted beam yield as a function of crystal motion in and out of the beam were more directly related to accelerator beam properties.

The following sections describe the E853 experiment, extraction techniques, kick mode behavior, beam halo effects observed through crystal and collimator motion, oscillations and modulations, rf extraction, fiber scattering, and summarize the conclusions. Other aspects of the E853 results have appeared in Murphy et al.¹, Ramachandran's thesis², Fermilab 97/300³, the recent Near Beam Symposium⁴. An earlier related study by Jackson⁵ was carried out before E853 to measure diffusion rates and collimator effects in preparation for the experiment.

2. The experiment

The E853 extraction experiment was straight-forward. The apparatus was placed at C0 where there was an existing Tevatron abort line (see Figure 1). Protons from the circulating beam were kicked or diffused outward to a bent crystal that deflected the particles upward by 640 μ rad. From there they traveled 100 m along a simple beam line to two diagnostic counter stations ("air gaps") separated by 40 m. Measurements consisted of determining the count rate down the beam line as a function of crystal alignment, strength of the beam halo excitation, and other parameters.

Each station contained several scintillators. For diffusion mode the scintillators were operated as single particle counters. Count rates were limited to somewhat less than the bunch passage frequency (300 Khz for 6 bunches). For kick mode a significant fraction of the circulating beam was extracted down the abort line so that counter voltages had to be lowered to avoid saturation. For that case scintillator pulse height was proportional to extraction rate. Three principal counter combinations were used. So-called U counters below and slightly downstream of the crystal were used to monitor interactions of the beam with the crystal. Two counters in the first air gap formed a coincidence AG1. This was often placed in coincidence with a counter in the second air gap such as CAL. Typically several scintillator signals were tracked for many turns after a kick with digital oscilloscopes. An accelerator segmented-wire ion chamber (SWIC) was installed in the second air gap. There was also a toroid in the second air gap to measure beam current. A fluorescent screen in the first air gap monitored the beam. Video tapes from the screen CCD camera were used to look at time dependent effects with scales greater than 15 ms in kick mode. Loss rates at the collider detectors were measured using permanent detectors located at B0 (CDF) and D0.

In the collider mode, the Tevatron typically operated with six bunches of protons and six bunches of antiprotons circulating so that a proton bunch passed the crystal every 3.49 microseconds. The RF bucket separation was 18.8 ns. A typical bunch length was 1 ns.

Characteristically the beam circulated in the Tevatron for many hours as the beam slowly decayed due to such factors as losses at the collision points, gas scattering, and scraping.

Under most circumstances the Main Ring Accelerator located just above the Tevatron was also operating to build an antiproton stack during collider operations. It cycled once every several seconds so it was possible to gate off detectors when protons were in the Main Ring. However magnetic effects due to bus-work and the magnet ramping affected Tevatron orbits throughout the Main Ring cycle.

3. Extraction techniques

Two techniques were used for extracting the beam in E853. In one approach a fast kicker was used to perturb the beam and increase the halo by several percent. This halo spilled out on the crystal over the next 100-1000 turns. The second approach was parasitic extraction relying on either natural or stimulated diffusion.

Kick mode was employed in the initial runs of E853. The basic technique was to move the crystal in to a pre-determined horizontal location close to the beam ($4-8 \sigma_x$ from the beam center). The beam was then kicked transversely several times by a fast kicker at E17 (see Figure 1). This kick led to a significant step toward the face of the crystal by the beam in the second turn around the Tevatron for one of the six bunches in the machine. After several hundred turns following the kick the beam had grown as non-linearities in the machine gradually spread the beam to fill most of the phase space mapped out by the betatron oscillations. This increased the beam emittance thereby "growing the beam." For kick mode the total beam extracted down the line was typically on the order of 10^9 protons/kick. The nominal value used for the kicker voltage was 10 kilovolts. The maximum step size at the crystal with a 10 KV kick was 500 μm .

In the "diffusion mode," the crystal was slowly moved into the tail of the beam halo. This parasitic approach did not seriously affect the circulating proton beam lifetime with the Tevatron running in the collider mode. Diffusion was due to such effects as beam-gas scattering, beam-beam scattering and tune shift effects, magnetic field ripple, and imposed RF noise. A special diffusion case discussed in a later section was driven by scattering from the passage of flying wires. Extraction happened over a long time scale, many thousands of turns, compared to several hundred turns in the kick mode. Much of the beam which did not channel underwent multiple scattering and got another chance to enter the crystal on successive turns. The most effective instrumentation for beam measurement in this mode was the scintillation counter system set at voltage levels for single-particle identification.

A horizontal damper located at F11 was also used in several E853 sessions to introduce RF noise in transverse phase space and thereby stimulate diffusion and increase the extraction rate. This characteristically decreased the beam lifetime substantially although it was still long enough for a typical study session. Significantly higher extraction rates were observed with the noise on. This approach could not be used for parasitic extraction due to its destructive effect on the circulating beam.

4. Kick mode time dependent effects

The major time structure in kick mode was due to accelerator beam dynamics. The nature of the E17 kick was such that the beam was on the inside of the ring on the first turn after the kick and only moved to the outside where it could strike the crystal on the second turn. On succeeding passes the beam moved back and forth across the aperture at B48 depending on the betatron phase. Multiple scattering of non-channeled particles in the silicon softened the process. This process has been successfully modeled in simulations prepared by Bogacz et al.⁶ and Biryukov⁷. As would be expected, the detailed microstructure of the turn-to-turn variation was quite sensitive to the accelerator tune. This was also observed experimentally for tune changes in different runs. Indeed, information on the micro-structure was more indicative of tune changes than underlying physics related to channeling.

Figure 2 illustrates the behavior for the actual data and the Bogacz simulation for the first 23 turns (about 400 μ s). In this time domain the extraction data rate based on the pulse height in a scintillator is reasonably modeled by the Bogacz simulation program except that extraction persists longer than predicted by the simulation. Not surprisingly, the detailed pattern from the Bogacz simulation is tune-sensitive.

Figure 3 shows the extraction pattern for a longer period (100 ms) for the large, right side buckets. The measured initial decay time (total) ranges from 0.6 to 2.5 ms. In that period the signal decreases by 10-60% for different kicks. Short values for this decay are more in line with the Bogacz simulation. It is difficult to produce $1/e$ times of less than 0.9 ms with the Biryukov simulation. Under somewhat artificial conditions that simulation can generate time constants of 2.0 to 2.7 ms. In the Biryukov simulation the decay time is relatively insensitive to the assumed interaction length, changing from 1.1 ms for a 30 cm interaction length to 1.3 ms for 45 cm. Horizontal misalignment leading to an effective dead layer also affects the fall time. For a 45 cm interaction length the fall time in the simulation increases from 1.3 ms when the crystal is correctly aligned horizontally to 1.5 ms for a 1 mrad misalignment, 1.7 ms at 2 mrad, 2.1 ms at 5 mrad, and 2.7 at 10 mrad. The fall time is quite insensitive to assumptions about the size of the kick.

A related issue is how long it took to reach equilibrium when the crystal was vertically misaligned. Multiple scattering due to multiple passes through the crystal is the underlying mechanism for this effect. Figure 4 shows the time distribution for forty turns after a kick for a -60 μ rad misalignment. Data sets were also obtained for -40 and -20 μ rad misalignments. Since the characteristic vertical angular divergence of the beam after several kicks was $\sigma = 30$ μ rad, the last case was almost within the envelope of the beam and should not have been so dependent on multiple passes to push particles to the right angle. The highest "right side" turn data (circle with an x) has been fitted with an exponential similar to a radioactive decay process. The form (dictated by available fitting routines) also effectively incorporates a time before any beam is extracted. At -60 μ rad no beam appeared for several turns. The rise time was 170 μ s or 8.5 turns. The asymptotic extraction signal was about 70% of the on-peak case. At -40 μ rad, the initial delay was still several turns and the time constant was 120 μ s. The asymptotic signal

reached the on-peak value. For $-20 \mu\text{rad}$ there was no initial delay and the rise time was one turn. A naive picture gives some insight into the process. On every pass through the crystal (approximately every other turn) the particle multiply scattered by $10 \mu\text{rad}$. To change by $60 \mu\text{rad}$ required 6^2 passes or 72 turns to full equilibrium while 30 turns were actually needed to get to 90% of the asymptotic value. Part of this difference was probably due to the effect of the beam divergence. With beam divergence and multiple scattering the time constant should go as Θ_m^n where $1 < n < 2$ and Θ_m is the misalignment angle. The Biryukov simulation reproduces the general features of the data but the simulation time constants are roughly twice as long ($200 \mu\text{s}$ at $40 \mu\text{rad}$ and $400 \mu\text{s}$ at $60 \mu\text{rad}$) and the pattern is not as smooth as the data. A wider effective accelerator angular divergence than used in the simulation might have led to shorter times.

Another related subject is the time for a "wrong side" turn to come out at the same rate as a "right side" turn. This equilibration is probably due to non-linearities in the accelerator lattice. Observationally the amplitude of wrong side turns remained small for 20 turns and then increased and came into equilibrium with the right side turns with a time constant comparable to the initial fall time for right-side buckets. This is illustrated in Figure 5. Neither of the simulations reproduces this feature since non-linearities were not included. Over several hundred turns in the Biryukov simulation the wrong-side turns remain small with no discernible pattern. The experimental data has been fitted with an exponential distribution coming into equilibrium with an asymptote. An effective initial delay before a signal of about $350 \mu\text{s}$ (18 turns) was followed by a rise with a time constant of $520 \mu\text{s}$.

A second interesting feature appears in Figure 3. This is a 10 ms period where the extracted rate hardly changed. The envelope decreased slowly at first and then more quickly. The initial slow portion extended for on the order of 20 ms. The time constant to the 50% point was 30 to 50 ms. The data hints that this might have been mixed in with some sort of 30 to 50 ms peak-to-peak oscillation (see later discussions under oscillations). Neither of the simulations is able to model this effect. Again, a plausible suggestion for a driving mechanism is a non-linear effect in the accelerator.

There were also effects extending out to many seconds after a kick. These were observed using video recordings at an effective rate of 60 frames a second with the CCD camera monitoring the scintillator screen in the extracted beam line. Three types of beam spot pictures were observed. One was the first frame corresponding to the left side of Figure 3. This was typically followed by several frames with "satellite" pulses of decreasing intensity corresponding to the decay portion of Figure 3. A third set of "volunteer" pulses was observed at times well separated from the initial kick. Since the CCD-scintillator system was quite non-linear it was not possible to make more than a qualitative judgement of the satellite or volunteer pulse intensity. The number of these pulses versus time summed over several kicks is shown in Figure 6 for all pulses (xs) and for the smallest ones (open circles). Note that this distribution is for the number of volunteer flashes, NOT the number of particles down the beam line. This distribution measures some convolution of the effect of small perturbations long after the kick with available halo generated by the kick that has not yet been scraped. The distribution dies with a time constant of 0.8 s. After five seconds there is an almost flat spectrum of very small volunteers.

5. Beam halo effects

Several E853 observations relate to the character of the circulating accelerator beam halo. The effect of retracting the crystal or a collimator a small distance sheds light on the diffusion rate of the halo. This rate is related to the beam halo phase space density and non-linear effects in the accelerator system. Likewise, the number of kicks required to move beam out to the crystal or "grow" the beam is an indicator of the halo density. Moving the crystal or a collimator generated related information. When the crystal was moved in there was an initial quick beam rise that died over several minutes followed by a sustained rate that could persist for hours.

Unperturbed beam lifetimes in the Tevatron are quite long. Typical proton beam lifetimes ranged from 70 to 90 hours, while the luminosity lifetime ranged from 11 to 18 hours. Because diffusion rates were long and data collection time was short, little data was taken where the incremental retraction of the crystal was small enough to produce a noticeable effect and the time interval before the next disturbance was long enough. Figure 7 shows the best information available from a diffusion run in collider mode. After a 200 μm pullout the count rate dropped by a factor of 4 then increased with a time constant of 2.2 minutes. Weaker information for a 50 μm pullout shows an initial drop of a factor of 2 followed by a rise with a time constant of 0.24 minutes. For a 5000 μm pullout the count rate dropped precipitously and there was no rise even after 20 minutes. Based on this information it is difficult to speculate on whether the time constant is linear or goes with the square of the pullout distance.

Studies of the time to reach equilibrium after a collimator move were complicated by relatively quick collimator changes with few measurements taken between adjustments. Characteristically all three collimators were moved at one time. In two studies the yield did not go up initially until the collimators were withdrawn by 250-500 μm . The effect of opening the collimators is illustrated in Figure 8 where the count rates at different collimator settings are plotted as a function of time. Typically there was a fast initial rise of less than 30 s shown by the gaps between settings at different collimator values. Other rate monitor information is consistent with an initial rise of less than a second. The rate of growth after the initial rise was on the order of $(1/x)dx/dt = 0.035 \text{ m}^{-1}$. This is a poor determination since the rise is relatively small and the time interval is poorly measured and recorded.

Somewhat related information is provided by measurements of the number of kicks required to move the edge of the beam out to the crystal. Typically it took 3-5 kicks to grow the beam. The kick voltage was normally 10 KV. Unfortunately no systematic data were taken to study how the number of kicks depended on the separation between the beam and the crystal. Figure 9 shows the behavior as a function of kick number for a typical case when $X_{\text{gon}} = -850 \mu\text{m}$ and the crystal to beam center distance was 3.54 mm.

Another related parameter is the time to reach equilibrium after the crystal was moved in. Normally there was only a short time interval available for analysis after the crystal was moved (typically 1-2 minutes) before some other change was made. Analysis was also blurred because the accelerator clock (read out to minutes) could only be interpolated to about 10

seconds. A surrogate for the relaxation lifetime rate was extracted by fitting a linear slope to get $-(1/n)dn/dt$. These data are shown in Figure 10 as a function of the goniometer x position (x_{gon}). No attempt has been made to factor out the actual beam position. A value of 0.4 means the rate will drop by 40% in a minute. Based on a 10 minute run during Run 29 this initial drop lasts on the order of 1 min. After the initial rapid fall over a minute or two the characteristic rate for luminosity on-off and the proton-only case dropped with a 1.5 hour decay constant ($1/e$). (Recall that the luminosity lifetime ranged from 11 to 18 hours.) Typically there is no statistical difference between a linear and an exponential fit for these long term halo decays. If the data from Run 24 (filled diamond) is disregarded one might make the case that the relaxation rate was small at large x_{gon} , increased until about $x_{gon} = 2300 \mu\text{m}$ to 0.3-0.4/min and then remained steady or dropped. Run 24 has high values at $x_{gon} = 3800 \mu\text{m}$.

6. Oscillations and modulations

In the course of E853 several different phenomena appeared that were initially ascribed to some sort of oscillatory behavior. The possibility of oscillations with periods on the order of milliseconds was investigated and none were found. All of the apparent effects were due to aliasing problems.

Similarly the possibility of extracted beam modulation due to the Main Ring was also investigated. There were real effects on the counters due to beam loss from the Main Ring, mainly at injection and extraction. However, these beam loss effects were gated out during the Main Ring acceleration phase. Initially there was concern that magnetic fields from the Main Ring or the associated busses would produce Tevatron orbit perturbations large enough to modulate the extraction rate. The possibility of Main Ring oscillations was studied by looking at volunteer pulses in the CCD camera as a function of the Main Ring cycle time after the kick. Figure 11 shows this distribution summed over the Main Ring cycle for several kicks. No statistically significant peaking in the distribution of the volunteers was observed. Coincidence counter data between airgap 1 and airgap 2 also gave little or no indication of Main Ring modulation.

One oscillation-like behavior was observed in kick mode studies. It is illustrated in Figure 3. The period between peaks was 30 to 60 ms. These oscillations were overlaid with the general decay of the signal after a kick. Only two or three maxima were observed because the scope trace was only 100 ms long. As a result it was difficult to make an analysis. If this is an oscillatory effect it might be related to synchrotron oscillations with a characteristic frequency of 39 Hz at 900 GeV or a sub-harmonic of the 60 Hz power.

7. RF-driven extraction

During several runs the impact of a transverse white RF noise signal located at F11 was tested. The effect of turning the RF on or off was almost immediate and had a very significant impact on the extracted beam. Unfortunately it was so significant that these tests were beset by

saturation problems in the counters. Nevertheless it is possible to make estimates of the time constants or upper limits on the time constants for some of these processes.

When the RF signal increased the scaler data (typically taken several times a minute) rose immediately, suggesting the rise time was less than a minute. Fast time plot information on rate meters rose over a 10 s period and probably somewhat faster, suggesting a time constant ($1/e$) of 2-3 s for 4.5 V_{rms} on the RF damper. This voltage would result in a scattering angle of $\Theta = 10^{-4}$ μ rad and a jump at the crystal of 0.01 μ m/turn. Assuming this resulted in a linear growth (rather than a \sqrt{n} diffusion process) it would take 6 s for a particle to move out to $5 \sigma_x$.

Information on the effect of turning off the RF damper or turning the signal down was also available from fast time plots. When the damper was turned off from 4.5 V the extracted beam rate decayed over a 15 s time period with a time constant ($1/e$) of about 5 s. Similarly increasing the RF voltage by a ratio of 1.4 resulted in a change in less than 5 s.

8. Extraction driven with a fiber scatterer

Asseev⁸ and others have suggested that an amorphous scatterer placed closer to a circulating beam might facilitate bent crystal extraction. During E853 an initial investigation directed toward this possibility was carried out using the Tevatron "flying wire" system located at E11 and E17. The results were both interesting and curious.

During collider operations at the Tevatron three 30 μ m carbon fibers called flying wires are rotated through the circulating beam at a velocity of 5 m/s about once every half hour. Each fiber passes through the beam twice. These are normally used to measure the profile and momentum spread of the circulating beam. The "prompt" time distribution of the particles scattered off the fibers is related to the beam shape at the time the wires fly. For $\sigma_b = 0.7$ mm at the wires the half width at half maximum of the counting rate distribution as a function of time should be 165 μ s.

The flying wires were carefully monitored during diffusion mode running in the latter part of E853. A digital sampling scope operating in the peak detector mode tracked pulse heights for both an interaction and an extracted beam scintillator. The wire signals were clearly visible in the extracted beam. They were also seen at CDF and D0 where the detectors were gated off when the wires flew. Indeed for E853, counts taken during wire flies also had to be stripped out of the data analysis.

The voltages on these scintillators had to be kept high since they were also being used for counting. As a result there was a significant possibility of saturation and photomultiplier power supply drain because of the instantaneous rates. The phototube bases were equipped with transistors to provide some protection against slumping voltages. Post-run analysis indicated the extraction detector should likely have been able to sustain the rates. However in view of the interesting and unusual features exhibited by the extraction detector this potential problem should be kept in mind. One reason to believe there were not saturation effects or slumping of the

phototube voltages is that the scintillators did show a plausible modulated microstructure. A second way to evaluate the possibility of saturation is to look at the ratio of prompt extracted and interaction signals during regular and flying wire running. Since the interaction detector rate was a factor of ten lower it should have saturated less. During normal running this ratio was 10. For a typical wire fly it was 17, in the opposite direction expected for saturation.

Protons in the beam interact with a carbon fiber in one of two ways. They can undergo nuclear collisions with characteristic scattering angles of $300 \mu\text{rad}$ or experience atomic multiple scattering with a scattering angle of $0.16 \mu\text{rad}$. The chance of a particle passing through the wire twice is about $1/4$. Since the multiple scattering was small relative to the beam divergence it probably resulted in little beam growth. For 10^{12} circulating protons on the order of 10^7 undergo a nuclear interaction with a wire. Of these on the order of 3% or 3×10^5 per fly have scattering angles small enough to remain within the accelerator and strike apertures far downstream like the crystal. For a typical fly 7×10^4 of the particles scattered by a wire were extracted by the crystal including the prompt and delayed portions of the signal (see next paragraph). For an extraction efficiency of 30% this suggests that on the order of 2×10^5 were striking the crystal corresponding to a large fraction of the losses around the ring. This is not inconsistent with the fact that losses were observed elsewhere such as at the two collider detectors.

A distinct feature of the flying wire data for E853 was that the extracted beam detector for the crystal aligned showed a delayed signal that started some milliseconds after the prompt signal and extended for tens of milliseconds (Figure 12). The overall length of the time distribution is reminiscent of the pattern from kick mode, reproduced in Figure 12 from Figure 3. For a $60 \mu\text{rad}$ misalignment the size of the prompt extracted signal was consistent with a normal multi-turn alignment distribution. However there was no significant delayed extraction signal. For the aligned condition the total delayed extracted yield was about six times larger than the prompt yield. The interaction signal also had a delayed signal but with a shorter duration. The delayed interaction signal was two times larger than the prompt interaction signal.

The observed behavior suggests that the prompt extracted and interaction signals from a wire were due to divergent trajectories from nuclear interactions striking the crystal. The delayed signals could have been due to multipass effects that continued over 500-1000 turns. Initially these scatters would have produced rather divergent particles so that the interaction signal was relatively larger. As time went on halo evolution might have favored the preservation of less divergent particles that still remained tightly collimated relative to the circulating beam so that the extraction signal dominated.

The prompt rise times for both the extraction and interaction signals was $400 \mu\text{s}$ (10-90%) (see Figure 13). If this had been Gaussian, it indicates a sigma for the beam of $240 \mu\text{s}$ or 1.2 mm. While this is somewhat larger the actual beam sigma at E11 it is not unexpected in view of various sources of broadening. However the FWHM for the extraction counter distribution is more like 1 - 1.1 ms. This could be reasonably interpreted as multi-turn broadening. The extraction signal $60 \mu\text{rad}$ out of alignment also has a similar rise time but is narrower and more

Gaussian-like suggesting that indeed multi-turn effects may be responsible for broadening the prompt, aligned extraction signal.

The falling side of the interaction rate distribution initially looks like a Gaussian but soon develops a long tail. The distribution has three exponential parts (see Figure 14); 1) in the interval 1 to 2 ms after the peak the decay time is 5 ms, 2) in the interval 2 to 4 ms there is a faster decay with a time constant of 2 ms, and 3) in the interval from 5 to 20 ms after the peak the decay time is 6 ms. These regions are quite distinct. It is possible that this decay distribution is in some way reflecting the actual nuclear interaction angular distribution with the longer times mirroring partial contributions from very small angle scatters. Similar effects would fold into the extracted distribution but would be further complicated by alignment considerations.

The rise and fall times for the delayed extraction signal are hard to characterize. They range from 12 to 26 ms with the highest ones occurring for the x' cases. The times for the second fly in each of the three cases are 20-25% longer than the first fly. On the other hand there is no indication from the prompt signal that the core beam diameter had grown after the first fly. The x and y distributions are about the same. For both the x and y cases the rise is approximately linear. The decay time ranges from 2 to 5 ms. This decay time is difficult to characterize because of other effects such as modulations.

Several features of the flying wire study are worth emphasizing. First there was a significant prompt extraction that occurred with a plausible efficiency. There was also an even stronger delayed signal that may have come from multipass effects. After many passes these particles may have been extracted with higher efficiency. The features of this data deserve further analysis and simulation.

9. Conclusions

Time dependent effects in the E853 crystal extraction experiment have provided interesting insights into several crystal extraction and accelerator beam halo phenomena.

In kick mode the major time structure was due to accelerator beam dynamics. The turn-to-turn microstructure was sensitive to accelerator tune and more indicative of tune changes than channeling phenomena. Following an initial decay the extraction signal was almost flat then dropped in the 30 to 50 ms region. Small, longer term extraction glitches occurred out to 5 seconds after a kick. Kick mode extraction was reasonably modeled by the simulation programs except for the long-term persistence and the fact that so-called wrong side turns came into equilibrium with right side turns after a time constant comparable to the initial fall time for right-side buckets. These effects may have been due to non-linearities in the accelerator.

The time for an extracted signal to appear in kick mode for a misaligned crystal was also studied. This possibility arose because of multipasses through the crystal and the associated multiple scattering. For a misalignment of $-60 \mu\text{rad}$ no beam appeared for several turns. The rise time after that was $170 \mu\text{s}$ or 8.5 turns. For smaller misalignments the times were reduced.

The time constants are consistent with the simulation and also with a simple picture of the process based on multiple scattering.

Other E853 observations related to the character of the circulating accelerator beam halo. Retracting the crystal or a collimator a small distance shed light on the diffusion rate of the halo. This rate was related to the beam halo phase space density and non-linear effects in the accelerator system. In a typical case after a 200 μm crystal pullout the extraction rate dropped by a factor of 4 then increased with a time constant of 2.2 minutes. On the other hand for a 5000 μm pullout the rate dropped precipitously and there was no rise even after 20 minutes. Based on this information it is difficult to speculate on whether the time constant for halo diffusion is linear or goes with the square of the pullout distance. After a collimator move there was a fast initial rise in less than 30 s followed by a slower rise on the order of $(1/x)dx/dt = 0.035 \text{ m}^{-1}$. Related information about the halo was also provided by measurements of the number of kicks required to move the edge of the beam out to the crystal. Typically with a 10 KV kick it took 3-5 kicks to grow the beam.

When the crystal was moved in the rate was found to rise instantaneously then relax in a minute or so to an equilibrium point with a much longer decay period. The relaxation rate was small for large x_{gon} , increased until about $x_{\text{gon}} = 2300 \mu\text{m}$ to 0.3-0.4/min and then remained steady or dropped. After the initial rapid fall over a minute or two the characteristic rates for luminosity on-off and the proton-only cases typically dropped with a 1.5 hour decay constant $(1/e)$.

Little evidence was found for oscillations and modulations beyond some indication of a weak modulation with a period in the range of 30-50 ms. This modulation could have been due to any of several effects including sub-harmonics of the line frequency or synchrotron oscillations. Little evidence was found of oscillations caused by the cycling of the Main Ring other than the characteristic background increases due to injection and extraction.

Use of transverse white RF noise from the device at F11 produced little interesting in the way of time dependent effects. Equilibrium was reached in less than ten seconds when the damper was turned on or off.

Among the most interesting time dependent observations was the behavior of the extracted signal from the Tevatron flying wires. Particles interacting with the wires were extracted with good efficiency. The resulting high rates clouded the observations because of concerns about counter saturation although post-run analysis indicated they should have been able to sustain the rates. A distinct feature of the extracted beam data was a delayed portion that started milliseconds after the prompt signal and extended for tens of milliseconds. The length of the time distribution was reminiscent of kick mode operation. The delayed extracted yield was six times larger than the prompt yield. The interaction detector also had a delayed signal twice the size of the prompt signal with a shorter duration than the extraction signal. The rise time for the delayed extraction signal ranged from 12 to 26 ms while the decay time was 2 to 5 ms. The falling side of the interaction rate exhibited a long tail with three distinct exponential parts. The

observed behavior of both the extracted and interaction signals suggests that the prompt signals were due to divergent trajectories from nuclear interactions striking the crystal. The delayed signals could have been due to multipass effects that continued over 500-1000 turns. The features of this curious data deserve further analysis and simulation.

E853 received important help from the Fermilab Accelerator, Research, and Computer Divisions in carrying out this experiment.

*Operated by Universities Research Associations, Inc. under Contract No. DE-AC02-76CHO3000 with the United States Department of Energy.

References:

1. C. T. Murphy et al., Nucl. Phys. and Meth. **B119**, 231 (1996).
2. S. Ramachandran, Ph.D. thesis, UCLA (1997).
3. A. Asseev, et al., Fermilab-Pub-97/300-E (1997).
4. C. T. Murphy and R. A. Carrigan, Jr., to be published, Proceedings of the Near beam Symposium (Fermilab-1998).
5. G. Jackson, Proc. of the 1993 Particle Accelerator Conference, IEEE V<?>, 402 (1993).
6. S. A. Bogacz, D. B. Cline, and S. Ramachandran, Nucl. Instr. and Meth. **B111**, 244 (1996).
7. V. Biryukov, Phys. Rev. **E52**, 6818 (1995).
8. A. A. Asseev, to be published (EPACS-Barcelona).

Figure captions:

1. Schematic of the Tevatron channeling apparatus. The bent crystal deflects protons up through the quadrupoles into the field-free region of the Lambertson magnets. The protons are detected with a system of scintillators in two air gaps separated by 40 m. The inset shows the location of the crystal extraction system, the fast kicker, the RF damper, and the collider experiments at B0 (CDF) and D0.
2. Extraction rate as a function of the turn number from the computer simulation and from the pulse height in a scintillator following a particular kick, renormalized to the simulation result for turn 2. Pulse heights of less than 30 units are indistinguishable from the noise. There are 10% fluctuations in the relative pulse heights from kick to kick. Agreement between the observations and the simulation is good in the early turns but extraction persists during later turns longer than the simulation predicts.
3. Main decay of the extracted beam signal after a kick. Note the initial quick decay, the flat portion, a drop over a 25 ms region, and then the reappearance that hints of an oscillation. The rate is normalized to 1 initially.
4. Time to come to equilibrium for a kick to a crystal misaligned by 60 μ rad. Solid circles are the "right-side" turns. The points with xs are fitted. The rise time constant is 170 μ s. The rate is normalized to the fitted equilibrium point.
5. Wrong side behavior. Extraction rates on each turn are plotted with the high "right side" pulses circled and the low "wrong-side" pulses marked with squares. The fitting curves are discussed in the text. The y axis shows the unnormalized scintillator signal.
6. Long term behavior of the extracted beam after a kick. The y axis shows the number of volunteer pulses as a function of time after a kick (crosses give the total number of the volunteers). The magnitude of the volunteer signals decrease with time so that later pulses are mostly small (open circles).
7. Effect of pulling the goniometer out by 200 microns on the extracted rate. The triangles are the differences between the equilibrium portion at later times and the initial portion. These are fitted with an exponential with a time constant of 2.2 minutes. The filled circles indicate points used for the fit.
8. Effect of opening the collimators. The initial rise is given by the gap between succeeding slope-fit intervals and was probably less than a second. The rate continued to rise with a time constant on the order of 30 minutes.
9. Kicks required to grow the beam. Characteristically this took 3 to 5 kicks. The extraction rate is normalized to the full extraction rate after the kicks.

10. Relaxation rate after the crystal was pushed in for different values of x_{gon} over four runs. Except for the Run 24 case (diamond), the rate tends to rise with decreasing x_{gon} . The rate may have flattened for $x_{\text{gon}} < 2000 \mu\text{m}$. (Run 24-diamond, Run 27-circle, Run 29-square, Run 30-triangle.)
11. Distribution of volunteer pulses over the Main Ring cycle (summed for several kicks). There is little indication of any significant effect of the Main Ring cycle.
12. Smoothed signals for a typical wire fly for extraction (filled dots) and interactions (open diamonds). The extraction rate has been divided by ten. For reference the extracted beam signal for kick mode from Figure 3 is reproduced here normalized to the flying wire extracted rate (solid squares).
13. Smoothed time distributions for a wire fly for the prompt signals from extraction (filled dots) and interactions (open diamonds).
14. Smoothed time distribution for the flying wire interaction signal showing three different regions of exponential decay.

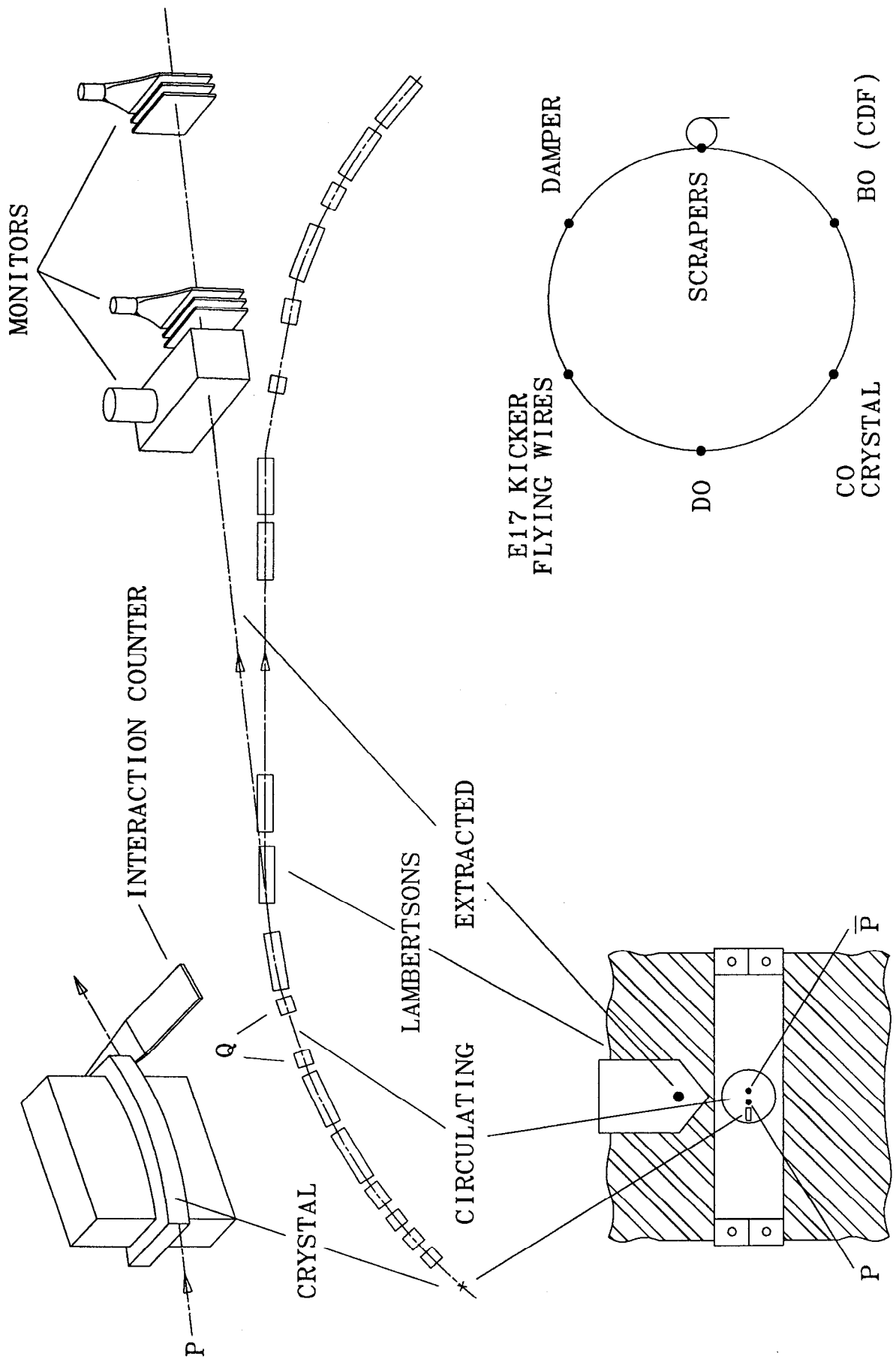
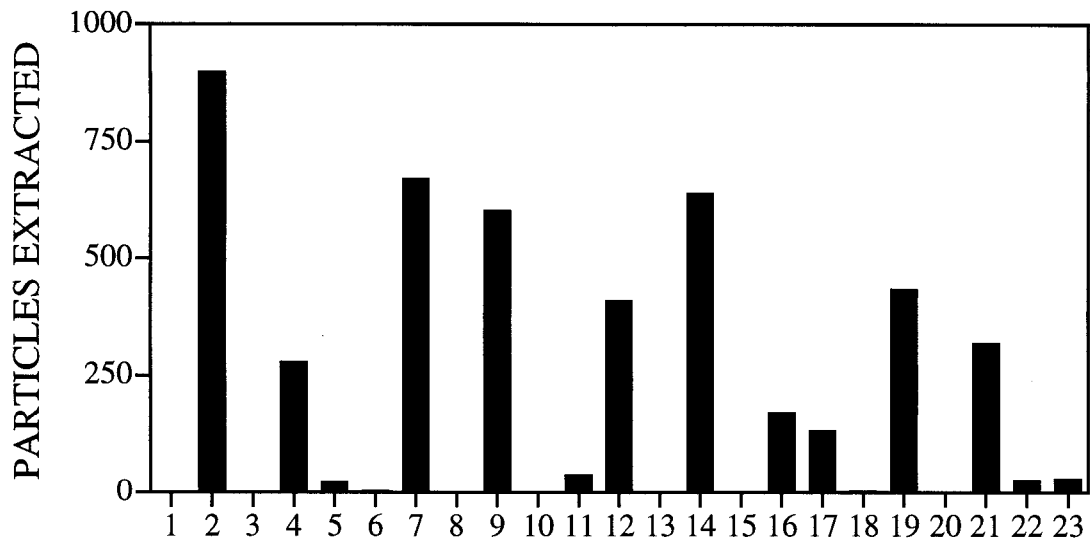


Fig. 1

SIMULATION



EXPERIMENT

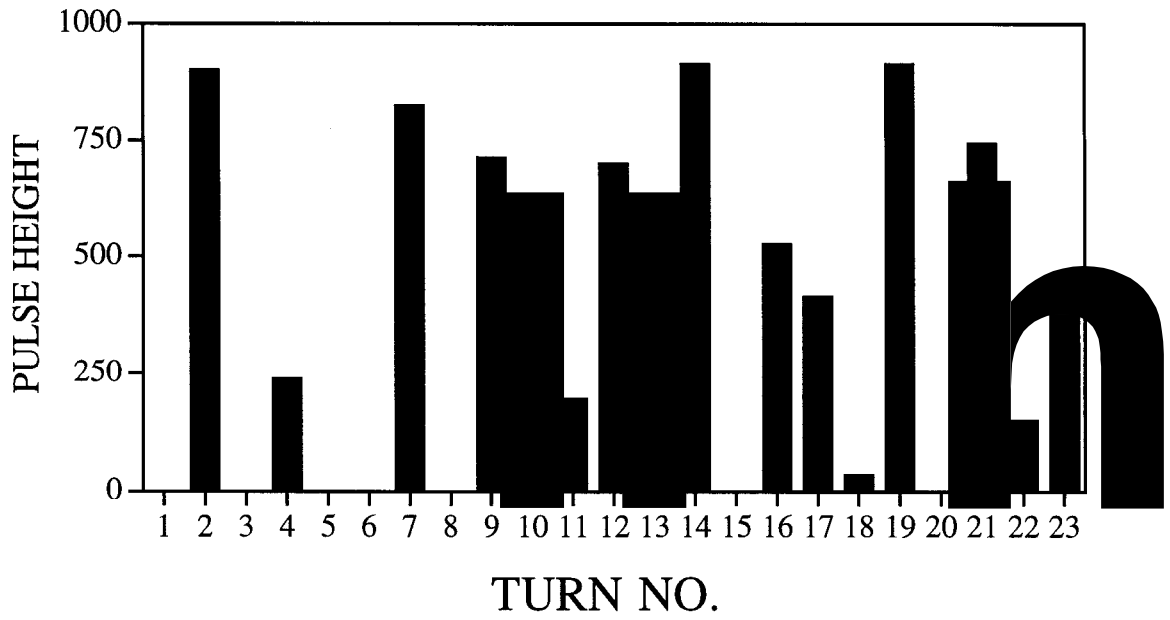


Fig. 2

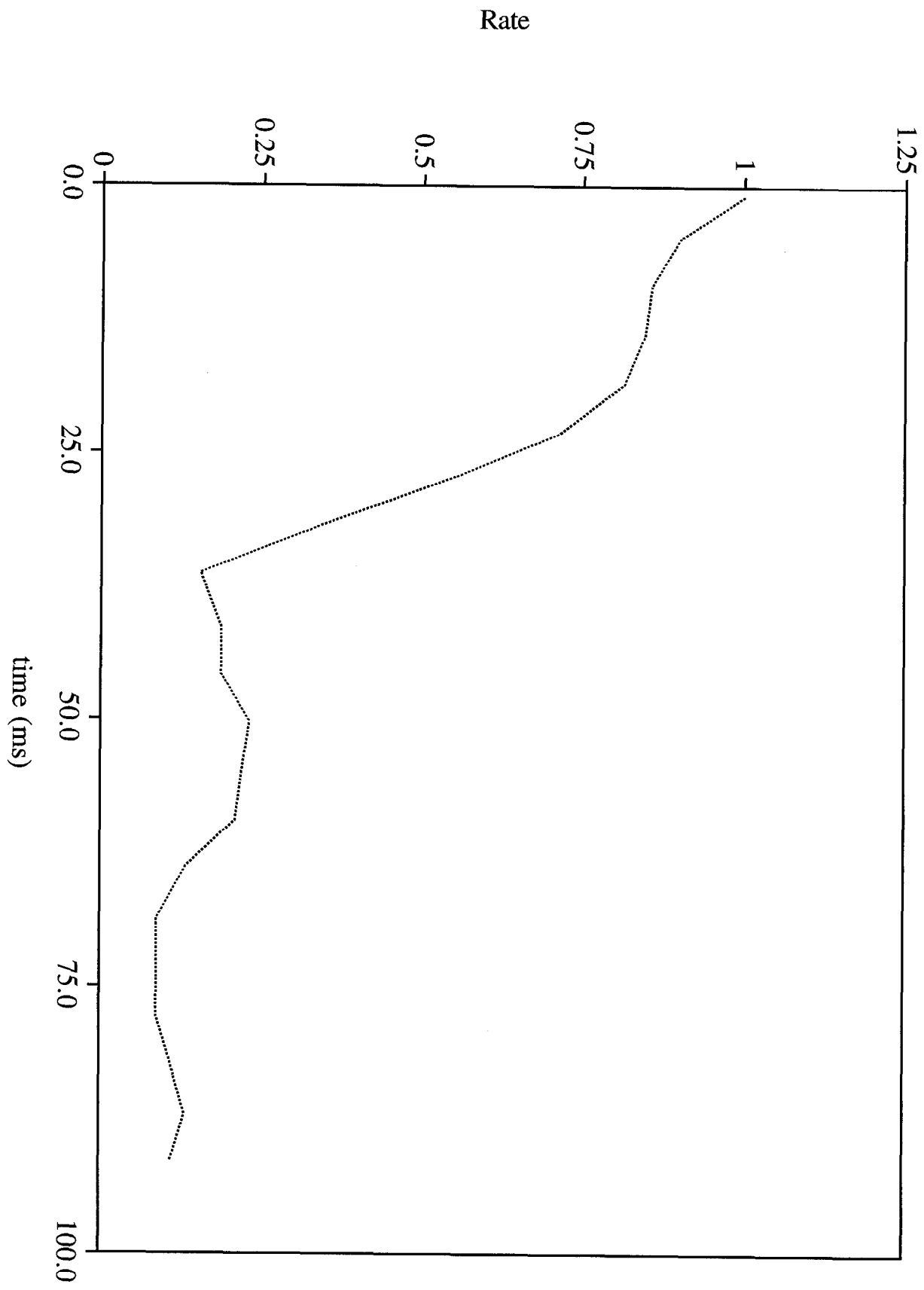


Fig. 3

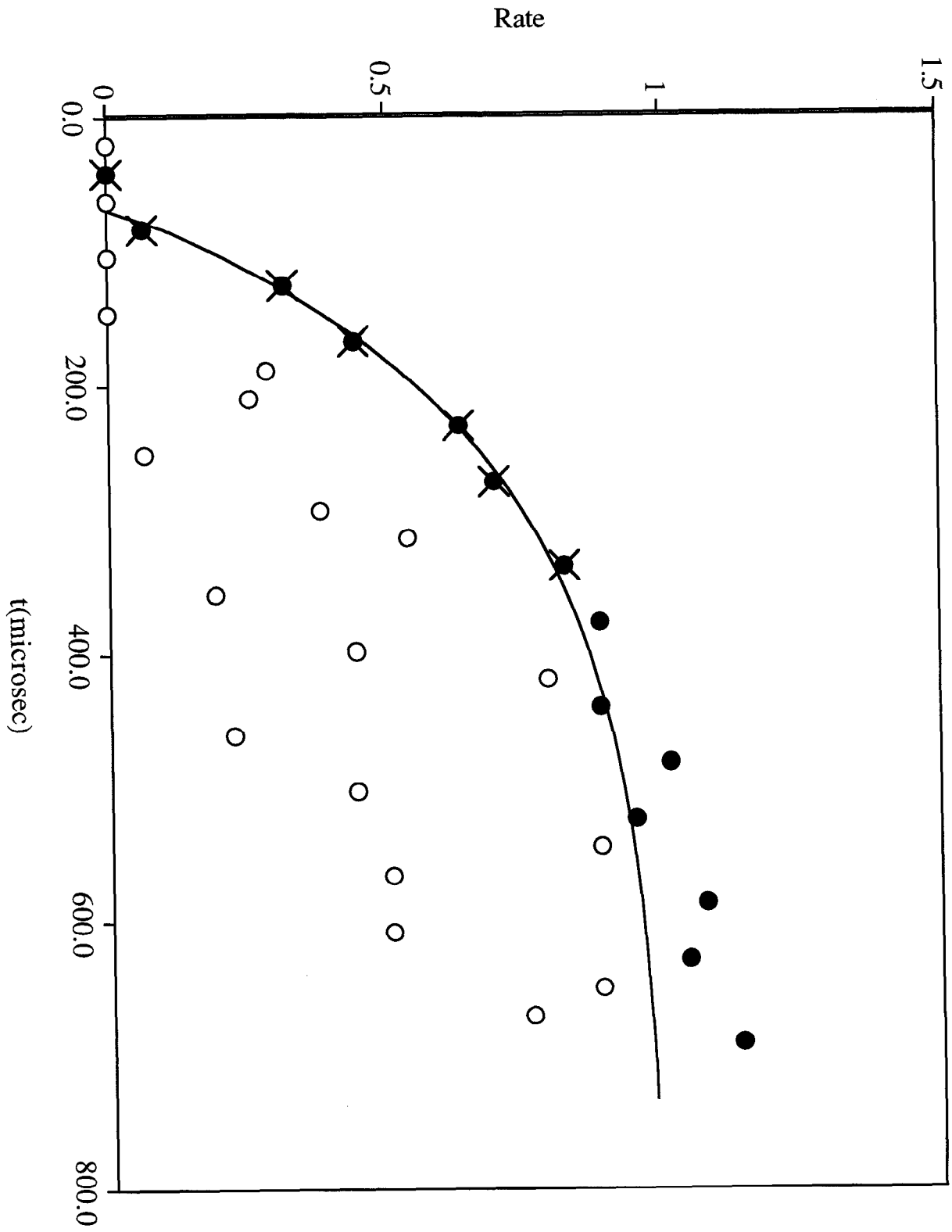


Fig. 4

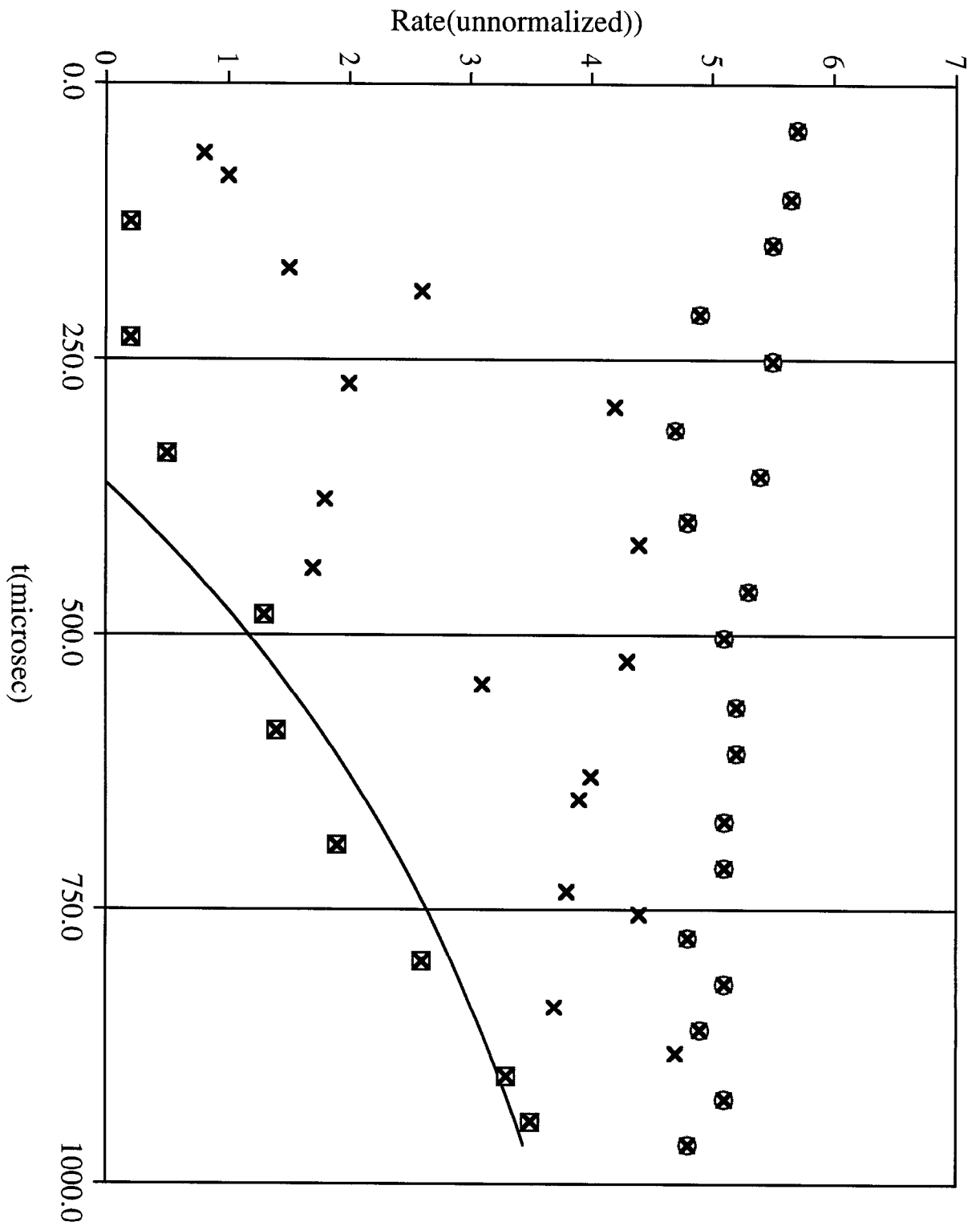


Fig. 5

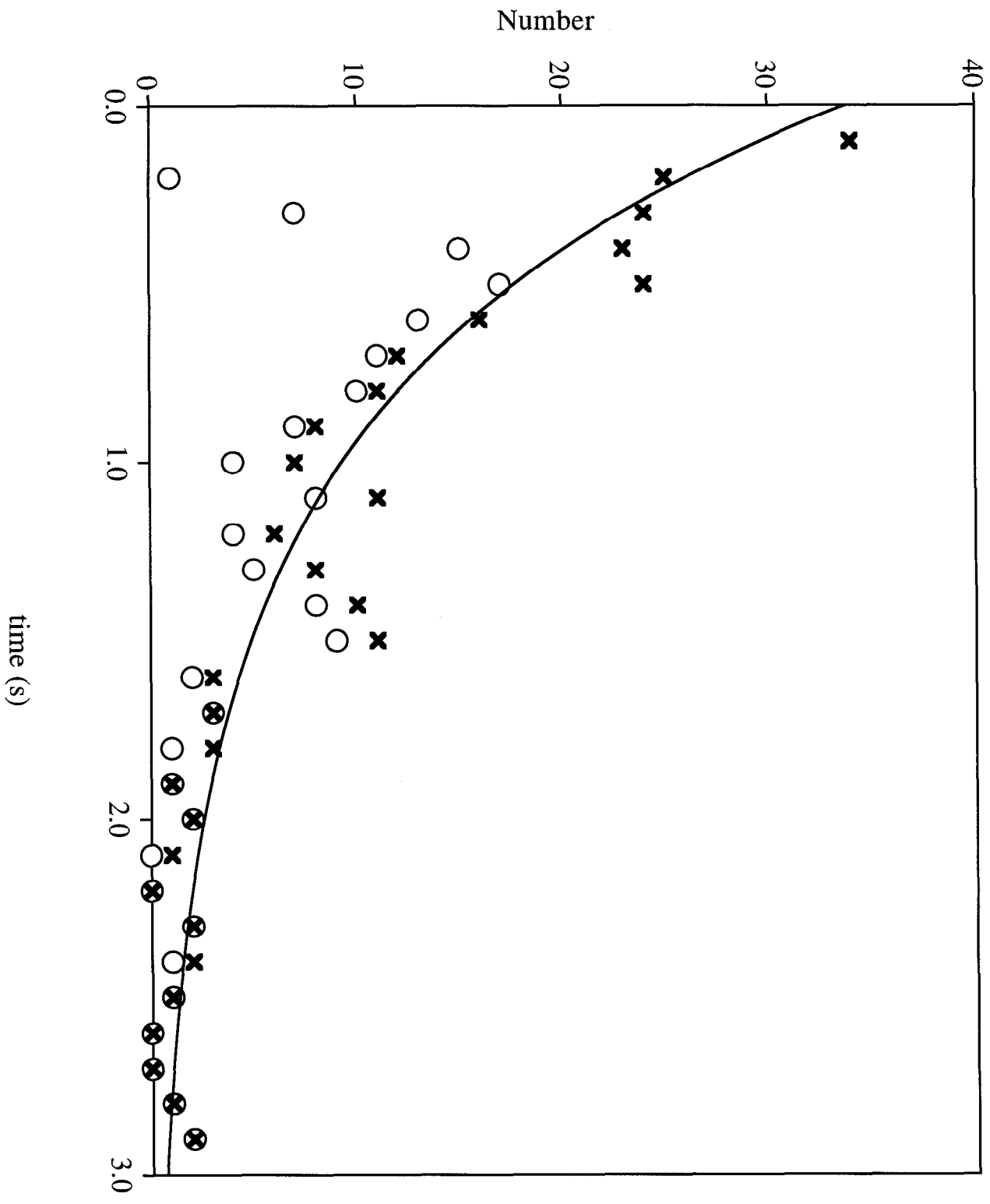


Fig. 6

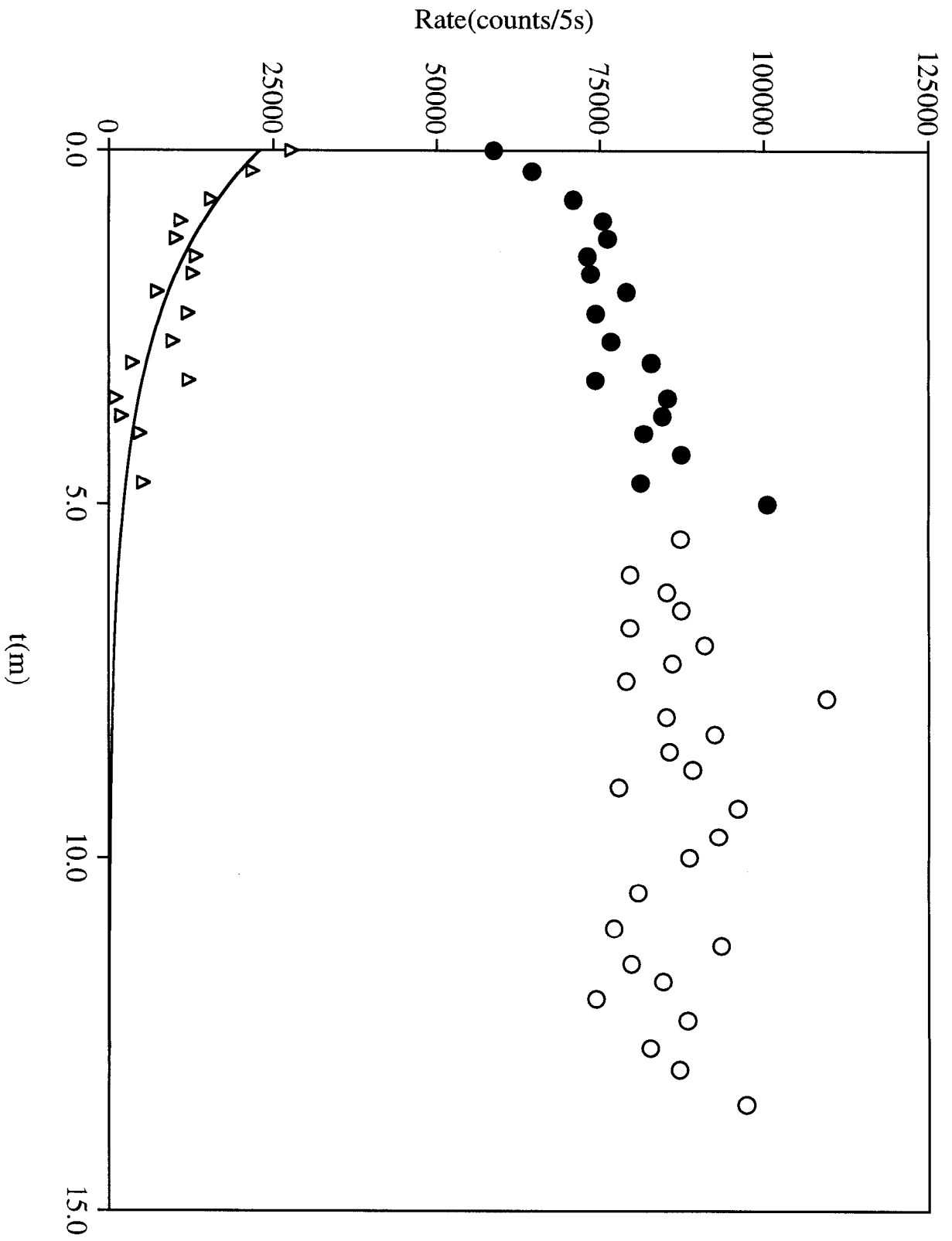


Fig. 7

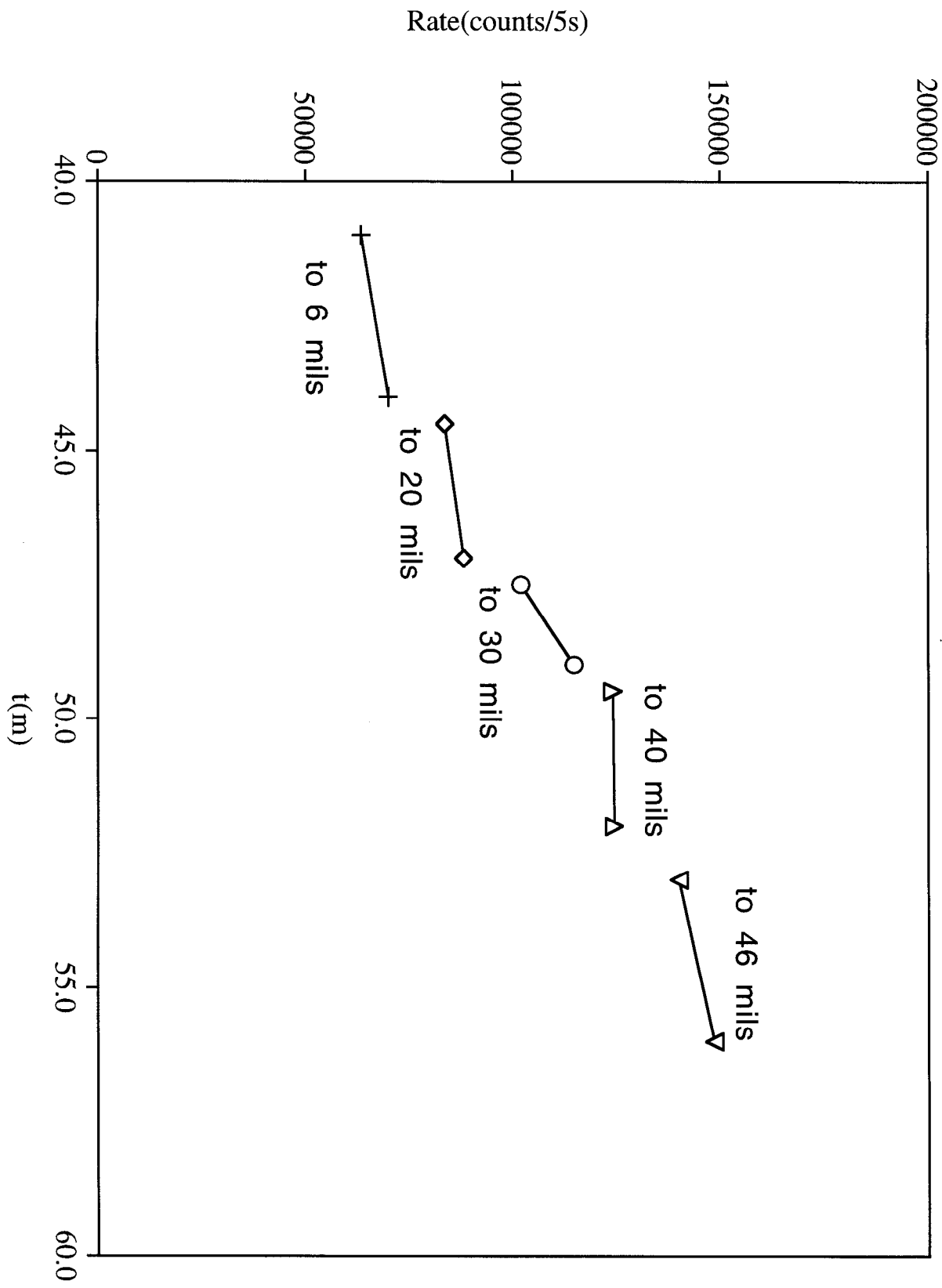


Fig. 8

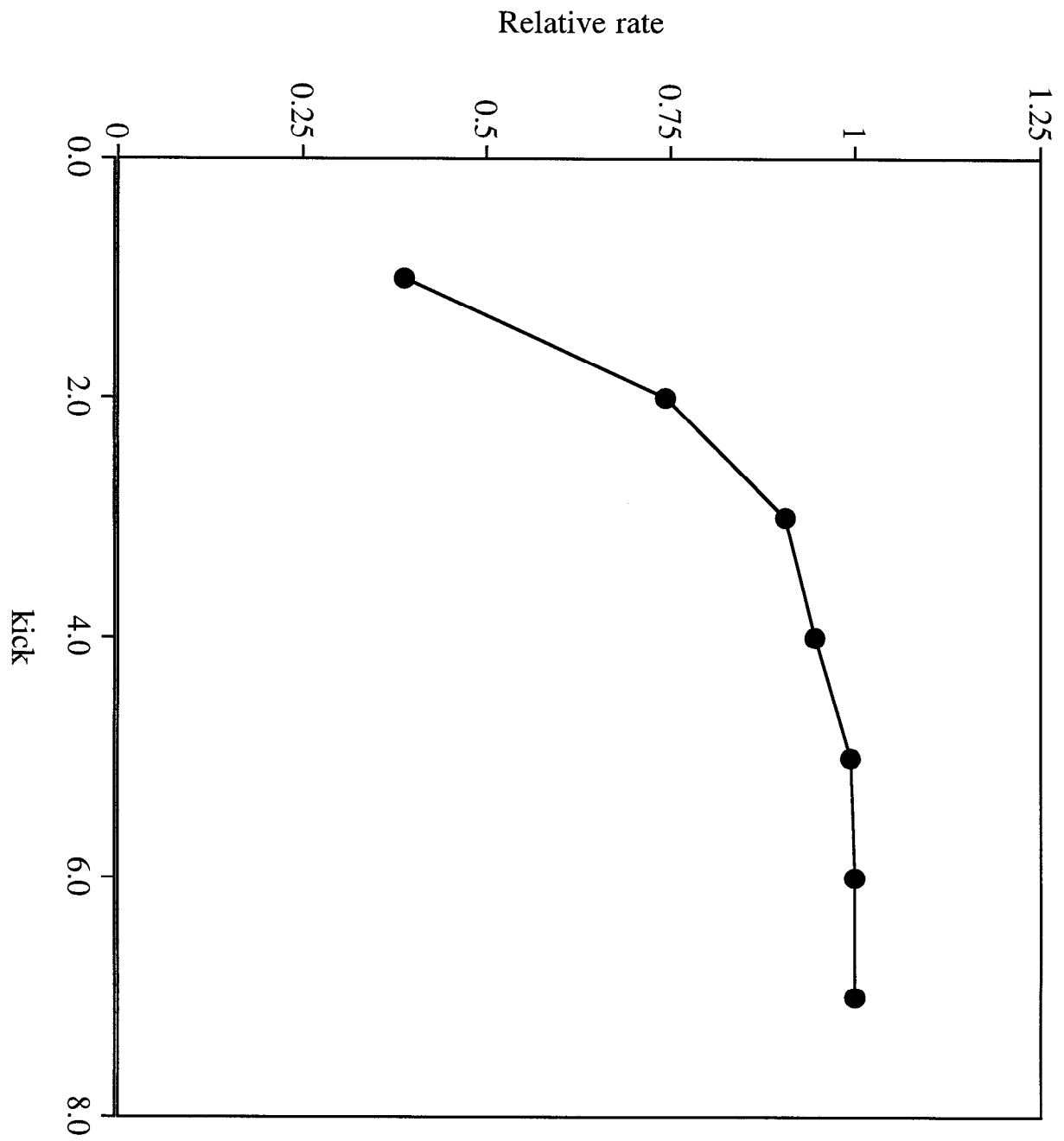


Fig. 9

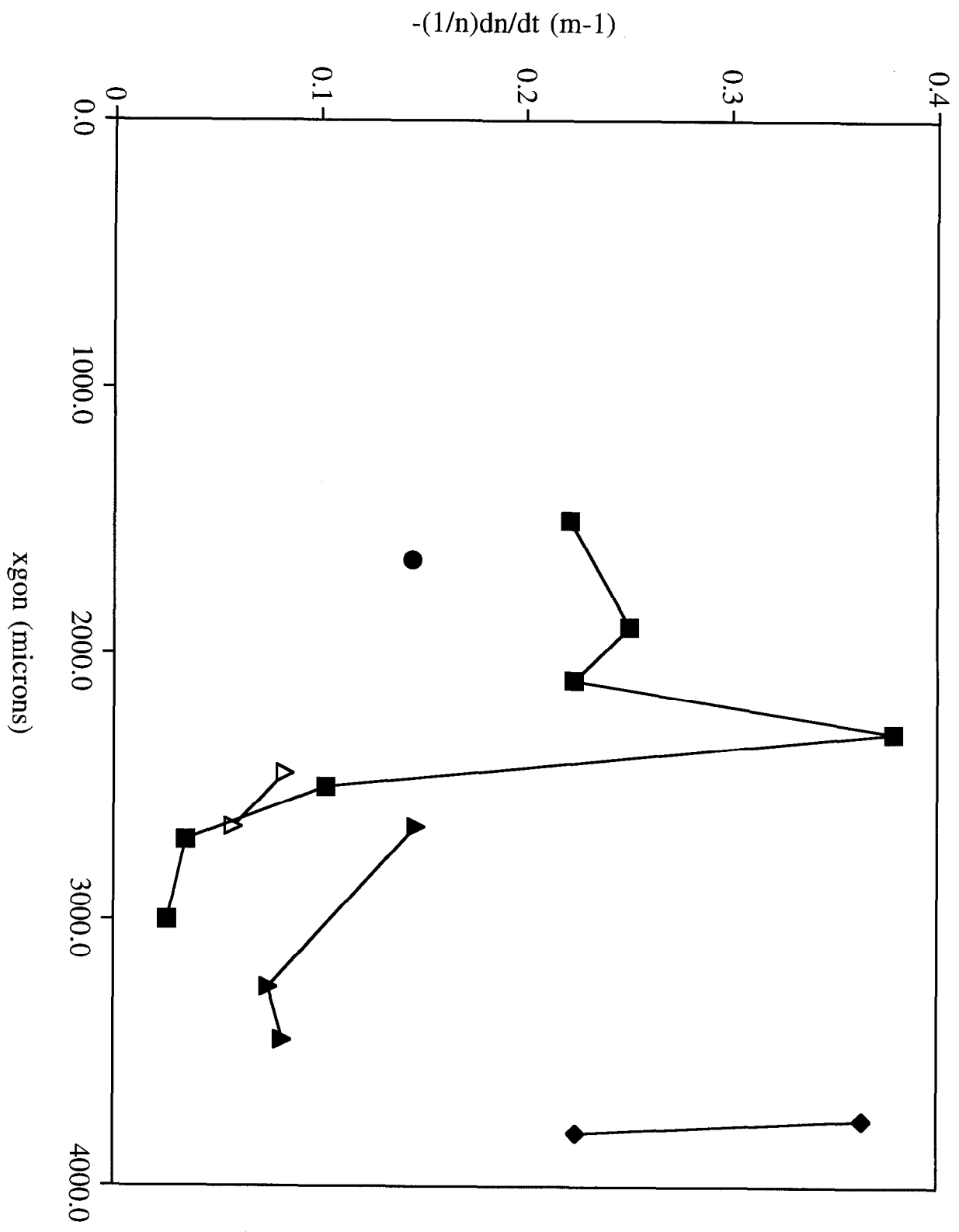


Fig. 10

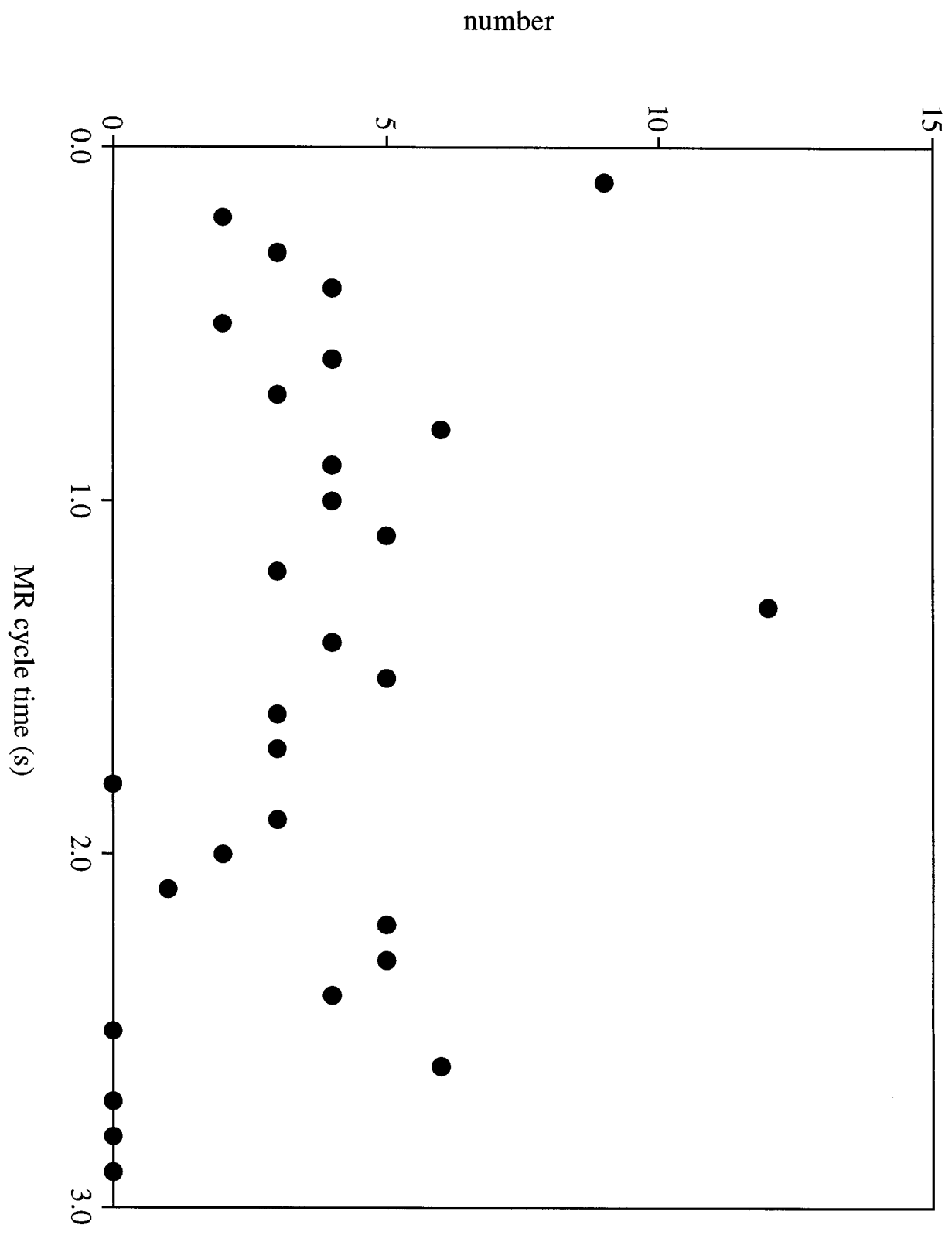


Fig. 11

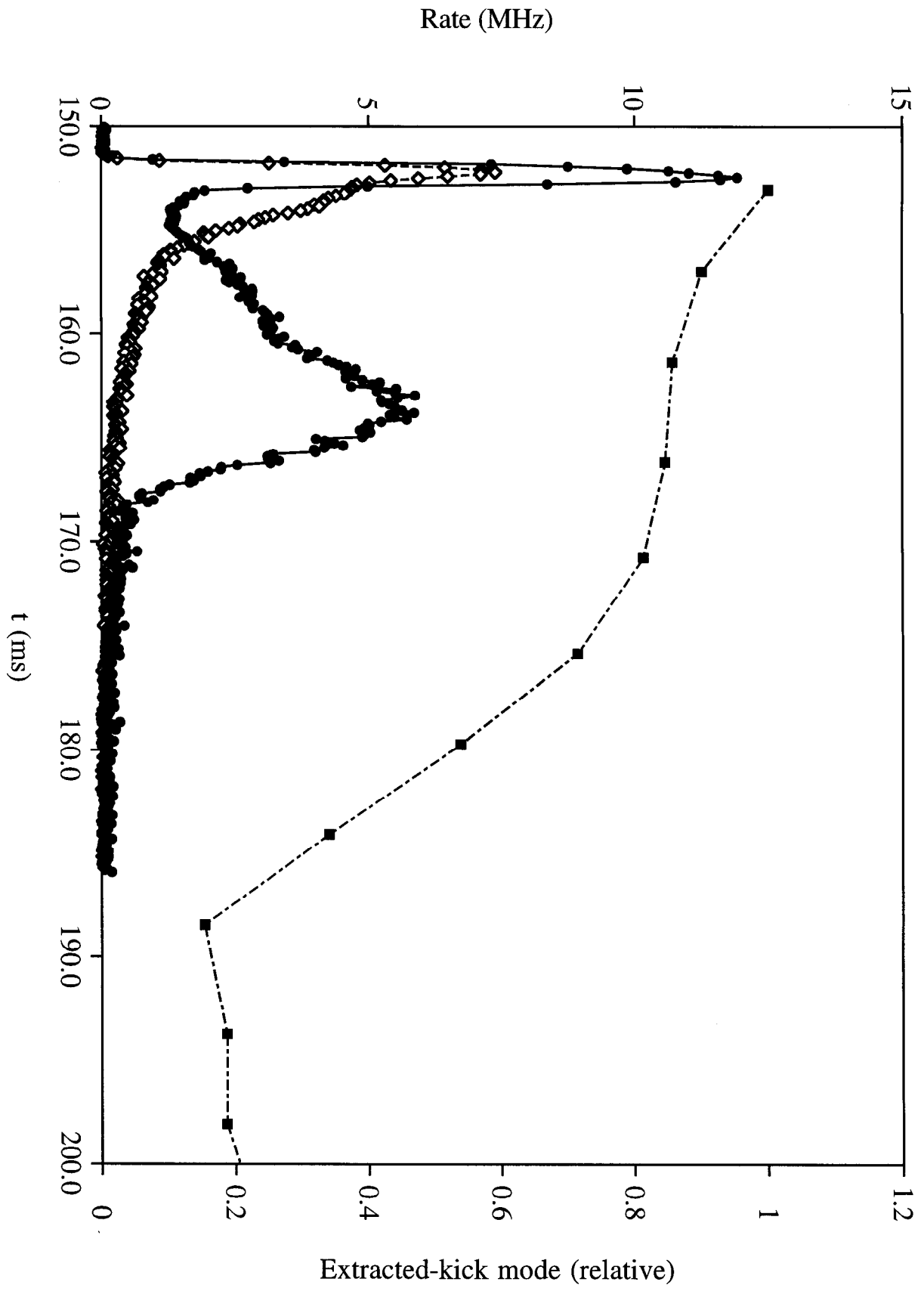


Fig. 12

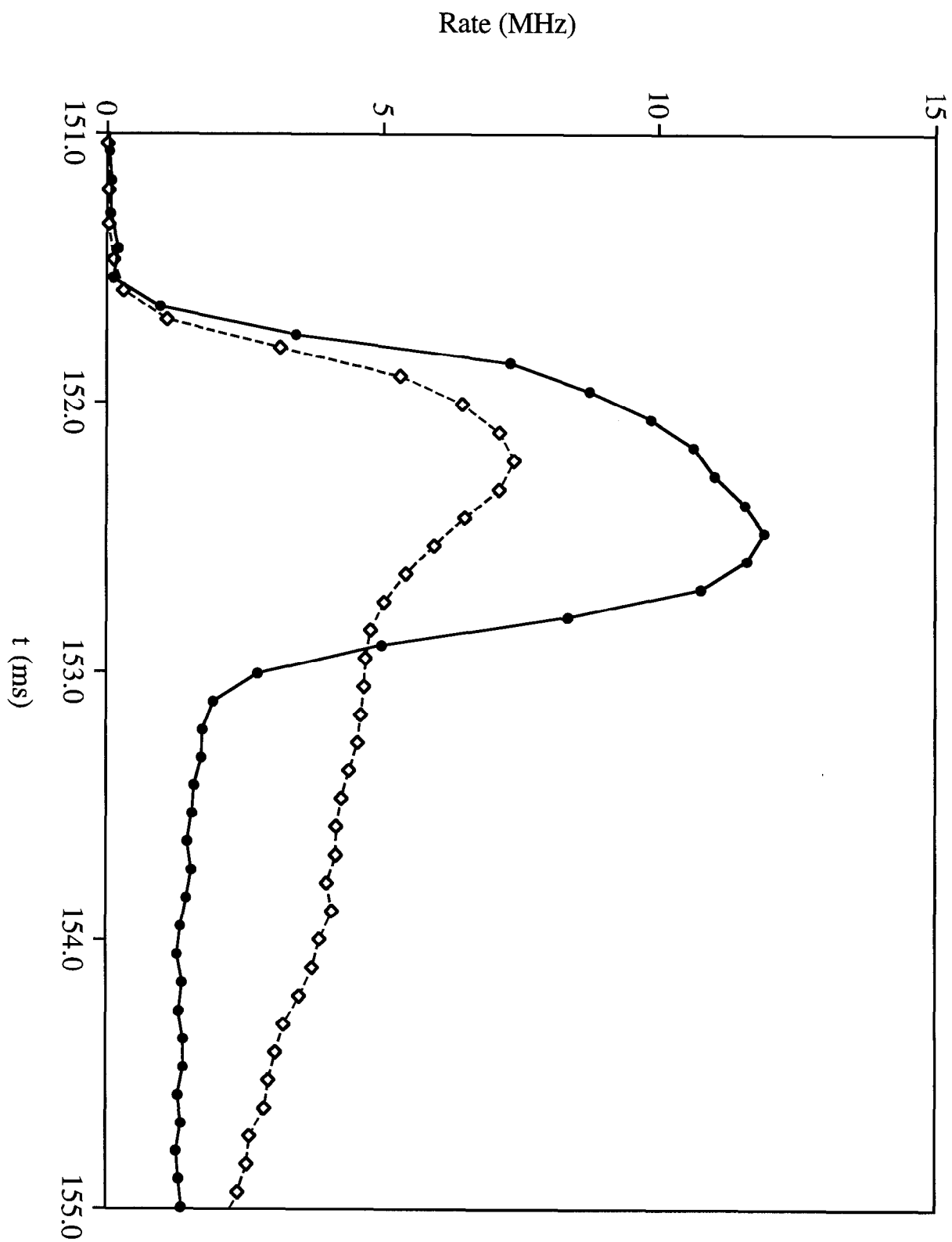


Fig. 13

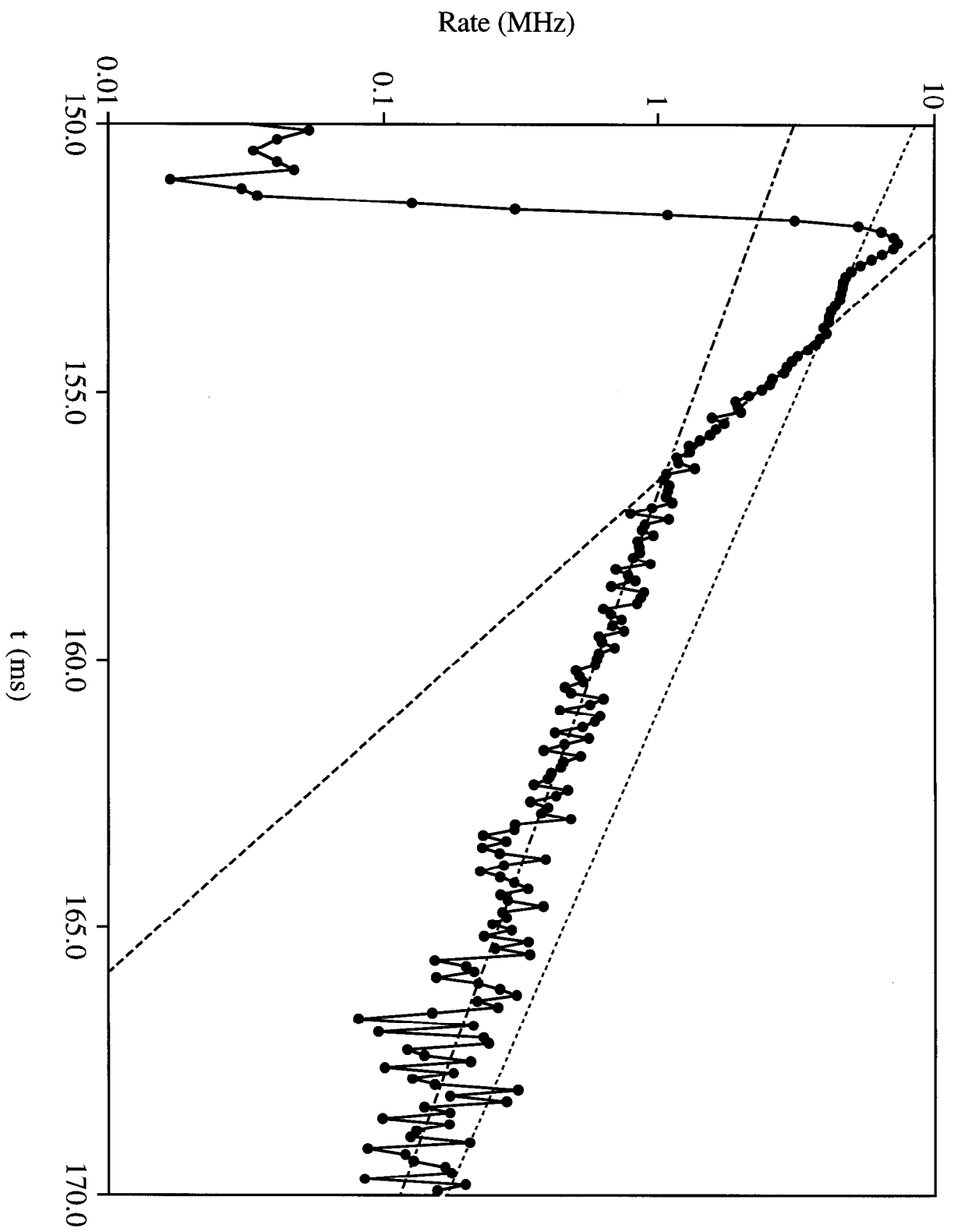


Fig. 14